Artificial Water Channels-towards Biomimetic Membranes for Desalination

Li-Bo Huang, Maria Di Vincenzo, Yuhao Li, Mihail Barboiu

Review
doi.org/10.1002/chem.202003470

Desalination |*Reviews Showcase*|

Artificial Water Channels: Towards Biomimetic Membranes for Desalination

Li-Bo Huang,[a] Maria Di Vincenzo,[b] Yuhao Li,[a] and Mihail Barboiu*[a, b]

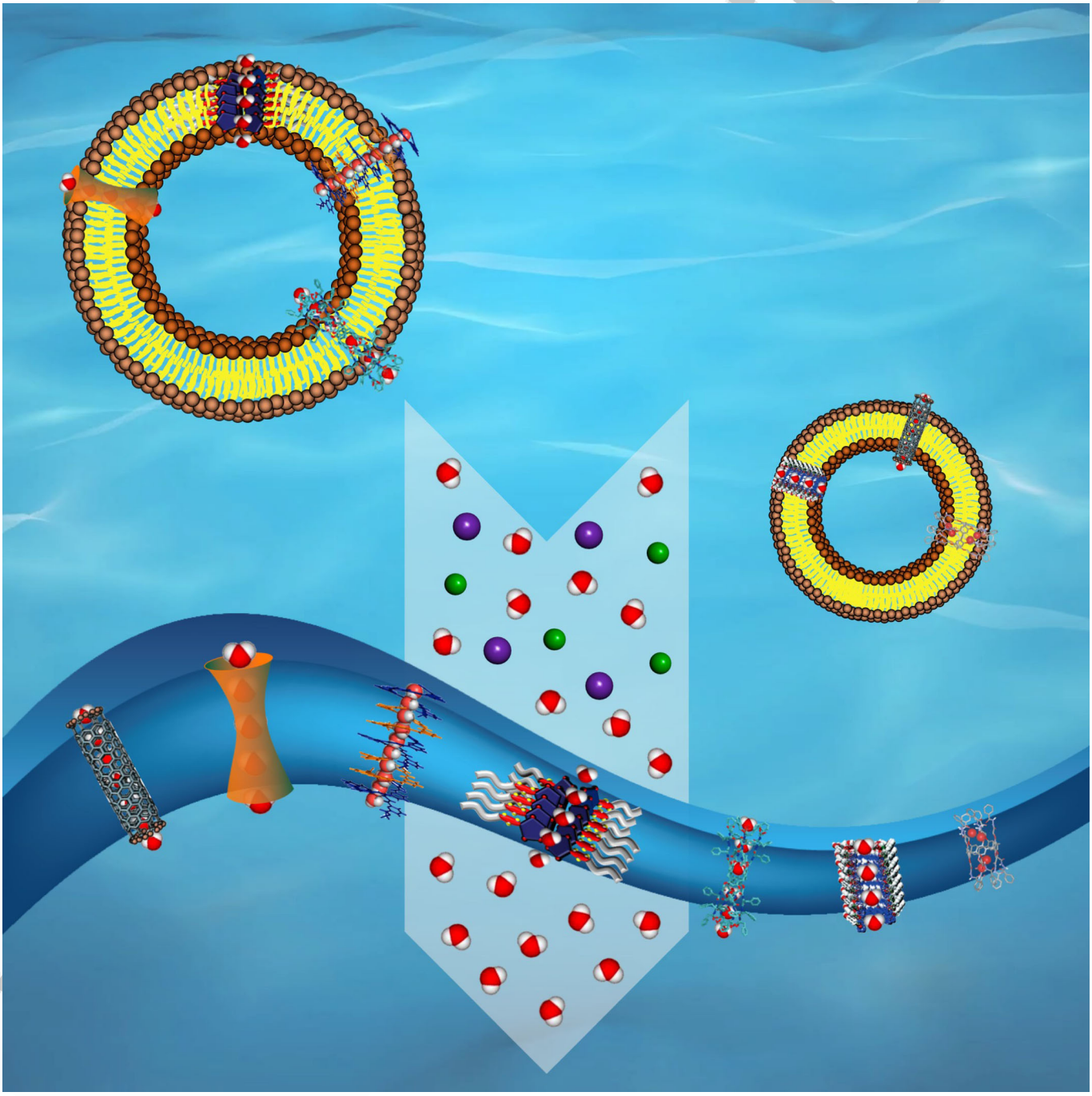

Abstract: Natural Aquaporin (AQP) channels are efficient water translocating proteins, rejecting ions. Inspired by this masterpiece of nature, Artificial Water Channels (AWCs) with controlled functional structures, can be potentially used to mimic the AQPs to a certain extent, offering flexible avenues toward biomimetic membranes for water purification. The objective of this paper is to trace the historical development and significant advancements of current reported AWCs. Meanwhile, we attempt to reveal important structural insights and supramolecular self-assembly principles governing the selective water transport mechanisms, toward innovative AWC-based biomimetic membranes for desalination.

Introduction

Water scarcity or the lack of the clean/fresh water is a highly important issue taking into account the actual synergistic growth of population and industrial activities.[1,2] To address the water supply requirements, membrane systems (MS) have been extensively explored during the few last years. Although seawater (SWRO) or brackish water (BWRO) reverse osmosis desalination are still expensive processes, their efficiency may be improved in the next years by modifying the technological process or by improving the membrane chemistry and composition leading to innovative structures and morphologies. There is a need for membrane innovation for which selectivity matters more than permeability.[3] Modern desalination technologies are using innovative materials with controlled porosity and morphology. Increasing the porosity of the membrane can easily lead to significant gains in both water and ion permeabilities with a detrimental decrease in selectivity. Specific water channels inserted in membranes can be used to improve the molecular interactions between water and conduits, providing selective water translocation through the membrane. Such a combination of robust polymeric matrix with selective AWCs will break the *permeability/selectivity* trade-off for channel-based scalable membranes (Figure 1).

Among such specific channels, AQPs are proteins known to transport water very fast with ion exclusion and are used for the fabrication of bio-assisted membranes. AQPs can be biomimicked by employing AWCs to assess the basis for biomimetic membranes for desalination processes. The objective of this review is to contribute to a better and deeper understanding of the natural and biomimetic water transport function and to discover new ways to generate advanced selective water desalination systems. To achieve this aim, different families of channels, materials, and membranes that maintain the highly selective water conduction activity, particularly those discovered in the last decade, will be presented. Toward this objective, this review will describe AWCs combining a particularly broad range of self-assembly and recognition features through hydrogen-bonding or hydrophobic effects, which play an important role in the ability to finely control the selective water translocation. Densely packed molecular/supramolecular AWCs may lead to an understanding of how such selective channels can be optimized at the nanoscale and incorporated within polymeric matrixes to facilitate ultrafast and highly selective transport of water at the macroscale through innovative membranes.

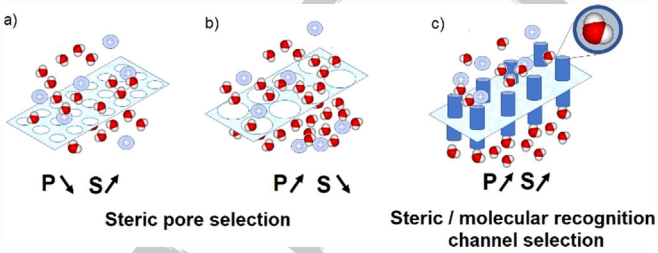

Figure 1. Permeability/selectivity trade-off for scalable membranes. Translocation/rejection governed by water–ion interaction through a,b) porous polymeric networks and c) selective channel superstructures.

Aquaporins and Porins

Natural systems developed over millions of years to evolve complex devices to translocate species across the cell membrane.[4] Biomimicry is a scientific strategy behind mimicking the well-tuned natural processes. Thus, nature should provide answers for efficient desalination.

Natural and artificial aquaporins

The most important natural water channels, the AQPs, are known to transport $\approx 10^8$–10^9 $H_2O\,s^{-1}\,channel^{-1}$ with perfect rejection of ions.[5–7] Structural information encoded within the hourglass-shaped structure of AQPs controls the efficient transport of water (Figure 2a): i) its selectivity filter (SF) with a narrowest diameter of 2.8 Å is adapted enough for water translocation, but restrictive to block the hydrated cations >3 Å, which is reinforced through electrostatic repulsion in the aromatic and arginine (ar/R) constriction region;[6,7] ii) a supramolecular water wire self-assembly occurs in the SF, adopting

[a] L.-B. Huang, Dr. Y. Li, Dr. M. Barboiu
Lehn Institute of Functional Materials, School of Chemistry
Sun Yat-Sen University
Guangzhou 510275 (P. R. China)
E-mail: mihail-dumitru.barboiu@umontpellier.fr
Homepage: http://nsa-systems-chemistry.fr/
[b] M. Di Vincenzo, Dr. M. Barboiu
Institut Européen des Membranes
Adaptive Supramolecular Nanosystems Group
University of Montpellier, ENSCM-CNRS
Place E. Bataillon CC047, 34095 Montpellier (France)
The ORCID identification number(s) for the author(s) of this article can be found under:
https://doi.org/10.1002/chem.202003470.
Selected by the Editorial Office for our Showcase of outstanding Review-type articles http://www.chemeurj.org/showcase.

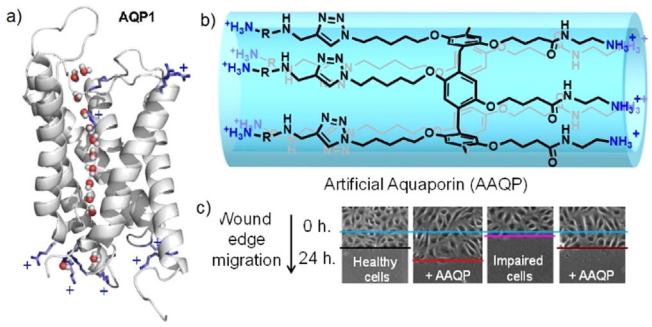

Figure 2. Structure of a) natural AQP showing the water wire channels as well as the positive charge at the entry and in the narrowest region of the pore and b) artificial AQP channels AAQP, with positive charges at the entry of the pillararene pore. c) Representative images of wound healing analysis of Chang cell assays showing wound edges (blue line) at 0 h (up) and 24 h (down) in the presence of AAQP (1.0 μM).

an bipolar orientation in two halves from the center to the entries of the pore. This creates an inversion central region, breaking the water wire dipoles, which inhibits the proton transport;[7a] iii) the positive charges at the entrance of the channel AQPs could further enhance the water transport activity owing to the reduction in the collective hydrogen bonding lifetime of the single water file;[7b] iv) water molecules form a "self-protecting" dynamic superstructure toward the exclusion of other species like H^+ or OH^-. Their inclusion favors disruption of the constitutive hydrogen-bonding network and energetically perturb the water self-assembly.[7c]

AQPs are essential for biological systems for their important function of regulating cellular osmotic pressure. The loss of function of AQPs could lead to some serious diseases, such as congenital cataracts and nephrogenic diabetes insipidus. Because of the simple passive and non-gating water transport mechanism of AQPs, it was also envisioned that the AWCs might be used to treat the AQP-related diseases by making the channels work as efficiently and selectively as AQPs in cell membranes. This possibility was firstly tested and achieved very recently by Hou and co-workers.[8] They have developed AAQP, an artificial AQP, which can work in cell membranes to allow its water permeability to reach that of AQPs with simultaneous ion and proton exclusion (Figure 2b,c). The elegant AAQP was constructed from tubular pillararenes, mimicking the key structural features of AQPs, including their positively charged channel entrances, hourglass-like cavity, single water wire file, and small constrictions to generate steric hindrance. It was revealed that the channel is functional in the cell membranes in a unimolecular manner, which is the best way to attain high channel stability. Interesting, the high water permeability of AAQP enables the restoration of the water transport of cells containing function-lost AQPs. Remarkably, the artificial AQP-mediated water transport can restore wound healing of the impaired cells that contain function-lost AQPs. This excellent work not only provided a simple model for chemists to investigate the influence of channel structures on the water transport and ion exclusion activities at the Ångstrom scale, but also developed a new strategy for the treatment of AQP-related diseases.

Porins

A significant number of studies have been dedicated to porins, which are a class of protein aquapores that form larger pores to transport ions, water, or small molecular solutes. Their structures show that their large pores are filled with clusters of water molecules in interaction with the walls of the porin

Li-Bo Huang obtained his BSc in chemistry in 2016. He is currently working under a joint PhD program in Chemistry of Materials at the Institut Européen des Membranes in Montpellier, France, under the supervision of Prof. Mihail Barboiu and at Sun Yat-Sen University in Guangzhou, China, under the supervision of Prof. Cheng-Yong Su. His research interests are the design and functionalization of AWCs and biomimetic membranes.

Maria Di Vincenzo holds a MSc in environmental engineering from Politecnico di Torino (Italy) and is currently a PhD fellow in Chemistry of Materials at Institut Européen des Membranes, France, working under the direction of Prof. Mihail Barboiu. She received the Nature Nanotechnology best poster award at the Dead Sea Water workshop 2019 (Ein Gedi, Israel) for the development of highly permeable and selective RO membranes incorporating AWCs.

Yuhao Li studied chemistry and received his PhD in 2018 from Sun Yat-sen University, Guangzhou, China. Currently, he is a postdoctoral researcher at Lawrence Livermore National Laboratory, CA, USA. His research interests focus on the development of AWCs/ion channels and biomimetic and bioinspired membranes materials.

Mihail Barboiu is CNRS Research Director at the Institut Européen des Membranes in Montpellier. A major focus of his research is Dynamic Constitutional Chemistry toward biomimetic membranes. He is the author of more than 300 scientific publications, 3 books and 22 chapters, and 400 conferences and lectures. Dr. Barboiu received in 2004 the EURYI Award in Chemistry and in 2015 the RSC Surfaces and Interfaces Award for the development of AWCs.

pores. The structures of bacterial Omp32 anion selective porin or OmpF porin present wider nanopores with larger diameters of approximately 10–20 Å.[7d] Their pores are completely filled with water molecules. Molecular simulations show that water diffuses more slowly than in bulk, probably owing to the strong structuration of water within the pores, similar to what is observed in carbon nanotubes (CTNs).[7e]

Bio-assisted protein-based membranes

During the last two decades, researchers around the world have been trying to capitalize on the unique properties of the AQPs in the design of bio-assisted membranes for desalination.[9] The natural proteins embedded in host polymeric membrane matrixes are active components for the selective transport of water. The question of how the AQPs and artificial host matrixes can efficiently work together has been answered.[9] Natural or engineered AQPs were first investigated by embedding them in protective amphiphilic polymerosomes. They exhibit a productivity of 167 $\mu m\,s^{-1}\,bar^{-1}$, that is, approximately two orders of magnitude more than a typical RO membrane with a productivity of 1 $\mu m\,s^{-1}\,bar^{-1}$.[9e] However, a such improvement in polymerosomes permeability at the nanoscale does not have the same impact when translated to the macroscopic membranes films embedding AQPs. Currently, the market of biomimetic membranes is represented by AQP membranes, in which natural AQPZ are embedded with proteo-liposomes and immobilized in the reverse osmosis (RO) polyamide matrix by interfacial polymerization (Figure 3a).[10,11] For these membranes, the major drawbacks are the protein stability and the vesicles rupture under the harsh conditions of SWRO ($\geq$35 000 ppm NaCl, 70 bar), which ultimately result in lower salt rejection values compared with marketed state-of-the-art RO membranes.[10] Most importantly, today no readily usable AQP-based membrane exists for SWRO desalination.

Overall, the challenges to use AQPs as the selective elements in bio-assisted membranes incorporating AQPs relate to their:

1) Long-term stability when embedded in vesicle-polyamide (PA) thin layers, which was demonstrated;[10e,f]

2) Bio-related processing and low resistance to SWRO (65 bars and high salinity 35 000 ppm NaCl) or BWRO (15–20 bars and salinity 3000 ppm NaCl) unconventional requirements; low pressure 5–10 bars RO applications are usually reported for these membranes. Under SWRO conditions an AQP embedded membrane shows a water flux of around 20 $L\,m^{-2}\,h^{-1}$, at least half of that observed for a SWRO membrane under the same conditions ($\approx$1–2 $L\,m^{-2}\,h^{-1}\,bar^{-1}$)[8■■ok?■■] and 98.5% NaCl rejection at 55 bar when using 32 000 $mg\,L^{-1}$, meaning a 91% increase of the water flux is seen compared with the reference thin-film composite (TFC) membrane without AQPs.[10b]

3) Production—membrane proteins are challenging to mass produce; however, production of 45 g AQP/100 L fermentation has been reported;[10]

4) The area of AQPs (9.0 nm^2) is very large in relation to the size of its Å-scale active water channel;[6,7]

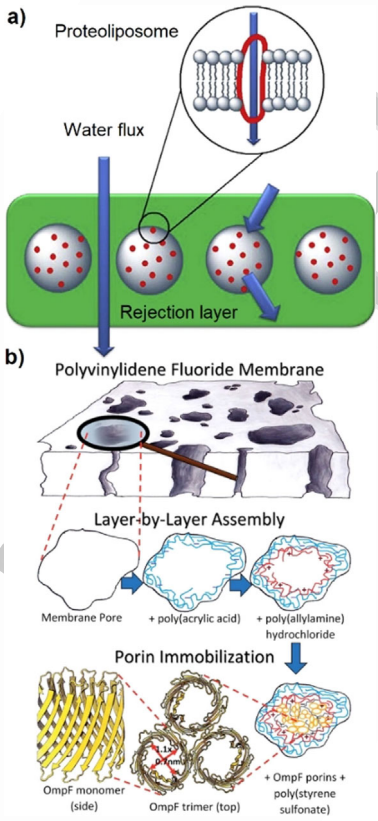

Figure 3. a) AQP-based biomimetic membranes, showing the AQP incorporation within proteasomes dispersed in a polyamide membrane.[10c] b) Layer-by-layer organization of polyelectrolytes into a PVDF membrane and stable immobilization of OmpF.[11] Adapted with permission from reference [10c], copyright © 2012, Elsevier and reference [11], copyright © 2017 Royal Society of Chemistry.

5) AQPs present a significant flux per channel, but not an acceptable permeability per active area, with a 25%[10c] to 83.6%[10d] to 166%[10e] increase in permeability for low-pressure (LP)RO or BWRO planar or hollow fiber AQP membranes, compared with the reference traditional TFC membrane without AQPs. Unfortunately, the NaCl rejection reached 97–98.5%, which remains a critical problem and defects created at the interfaces between vesicles and PA still have the leading performances of these RO membrane for desalination.

Other "porins" with larger pores of 7–11 Å, that is, OmpF protein trimeric channels from *Escherichia coli*, have been immobilized within poly(vinylidenefluoride) (PVDF) microfiltration membranes by poly-electrolyte layer-by-layer (LBL) self-assembly (Figure 3b).[11] The OmpF-selective membranes reject 84% of 0.4–1.0 kDa neutral organics over ionic solutes, which are transported two times faster than through traditional nanofiltration membranes. Different to AQPs membranes, the OmpF membranes are exceptionally stable, with constant high permeability and recovery for more than 160 h of filtration. This approach has been extended for larger proteins as building blocks with well-defined channel sizes that control the separation performances: $\approx$300–1000 $L\,h^{-1}\,m^{-2}$ at 1 atm and low solute concentrations $\approx$20 $mg\,L^{-1}$, with organic solute rejection similar to commercial nanofoam ■■definition ok?■■

(NF) membranes.[12a] On this basis, the scalability of the biomimetic membranes for future applications in desalination will need careful consideration to improve water/salt selectivity and to make use of the high permeance values of these membranes under BWRO industrial conditions, that is, using at least 15 bars and salt concentrations $>2\ g\,L^{-1}$.[12b] The OmpF membranes with higher porosity than AQPs membranes allow an impressive increase of water permeability with sharp and clear cut-offs at the nanometric level, but they failing in terms of the water/ion selectivity required for desalination. The optimization of both water permeability and selectivity remains important and is still a challenge when specific industrial operating conditions with concentration polarization challenges are employed.

Artificial Water Channels: Synthetic AQPs

As an alternative, chemists have attempted to replicate natural systems by using synthetically accessible and low-cost materials with an elegant combination of simplicity and utility. A possible alternative to AQPs are the synthetic biomimetic AWCs. Biomimicking the biostructures of proteins at the molecular level is an important challenge. A similar impact of water conduction activity obtained with natural AQPs can be obtained by using simpler artificial compounds displaying selective and high water transport functions like the natural ones.

The first biomimetic I-quartet channel was discovered in 2011[13] whereas the term "Artificial Water Channels" was first proposed in 2012 independently by Barboiu and Hou.[14] Amazingly, there was little or no systematic progress in the area of AWCs before this period. Within this context, biomimicking AQPs by using AWCs is an important endeavor from a) a fundamental science perspective, related to the deeper understanding of the relationship between the structural organization of water and its dynamic translocation under confined conditions through the channels and from b) an applied science perspective, as AWCs might have a huge impact on improving water filtration performances by using natural strategies to implement new paradigms for desalination.

Highly permeable AWCs may provide a route to producing efficient biomimetic membranes at laboratory and industrial levels, particularly for desalination. AWCs offer an effective and economic alternative to natural water channels.[13–17]

AWCs are synthetic ion-rejecting channels mainly consisting of unimolecular or self-assembled columnar structures, presenting a central hydrophilic or hydrophobic pore, to ensure the directional translocation of water, and an outer hydrophobic exterior matching the lipid bilayer or polymeric membrane environment.[14] AWCs offer the unique opportunity to set up high-performance systems with both high water permeability and completely selective rejection of ions. Recent results have made possible the production of AWCs, which feature efficient permeability of water, but their selectivity issues remain, in most cases, still unsolved. Having an artificial nature, the AWCs present the following important advantages:

1) their structural design is simple and they are easily tunable to be optimized for higher water recognition;

2) they can be synthetized in large amounts and at lower cost than biological counterparts;

3) their engineering scale-up becomes simpler and more reproducible without bio-related processing steps, they should be easy to include in membranes without the use of specific additives;

4) they are robust and stable when incorporated into membranes. We know that the active cross-section area of the AWCs is less important than that of AQPs, which increases their permeability per membrane surface area compared with AQPs membranes.

Most of the studies in the last decade on AWCs describe their synthesis, molecular modelling, and transport performances through lipid bilayers. Naturally, the inherent comparison of AWCs performances with those of AQPs appear to be restricted to specific research during that period. The water permeability of AWCs is from 2–3 orders of magnitude lower than that of AQPs, to similar or even better permeability for some AWCs; however, a major drawback is their low ion selectivity. Meeting the standard natural performances, discrete AWCs with are more stable for easy processing,[18] although their incorporation into large-scale membranes strongly depends on material design considerations and fabrication methods.[11] Among the promising material design approaches, Langmuir–Blodgett, vesicle rupture, pore-spanning, layer-by-layer techniques or interfacial polymerization have been used to form biomimetic membranes.[19] All these methods employ reconstituted channels in lipid bilayers or block copolymers as a strategy to preserve their integrity and functionality in the host membrane, which poorly rejects hydrophobic solutes. However, the formation of defects along with the functional modifications of the channels suggest that direct introduction approaches must be explored to better control the interactions and the compatibility between functional water channels and the surrounding membrane matrices.[20]

The specific structural design of selective channels is highly related to how we are able to construct such structural behaviors, to be able to selectively pump water like AQPs.[13,14] Therefore, there are incentives to further include these specific selective filter sites, which will increase the chances to attain improved selectivity for water through selective recognition and not by size restriction, rejecting ions and neutral molecules.

The two main challenging future endeavors for AWCs are:

1) to design perfect highly selective channels rejecting salts, allowing the preferential translocation of water;

2) the scale-up of the AWCs from the molecular level to that of macroscopic materials and meter-scale membranes.

Although this has been already proved by using AQPs,[10] no reports have been reported yet on using the AWCs within active layers for industrial membranes. To compete with RO technology, the current industrial standard for water desalination, water flux and salt rejection for AWC membranes need to be as high as that of natural AQPs. Higher flux values do not have an economic impact on desalination performances; however, it may improve the quality of the produced water by removing pretreatment processes. Preparing adaptive polymeric membranes able to host active AWCs are crucial for the future

of the next generation of membranes for desalination. The performances of lipidic or amphiphilic polymeric membranes as well as the classical RO polyamide materials can be diminished by organic molecules or surfactants present in water.[20] For the AWCs, the use of amphiphilic additives is not a necessary option. However, the study of AWCs in bilayer membranes is particularly important, as their performances need to be referenced to those of AQPs. Industrial application will certainly require polymers with a good mechanical robustness better than the lipid bilayers. It is important to know that the self-assembly and dynamics of channels may strongly depend on the nature of the hosting matrix and certainly their performances would depend on their interactions with external matrices. The structural self-organization of the channels within the polymeric matrix and that induced by external stimuli leads to variable materials with interesting adaptive behaviors, which cannot be totally predicted. In such scenarios, the predictive self-assembly of the channels in different matrixes cannot be described by specific chemical engineering equations. Chemistry would better mediate on a molecular level the dynamic self-assembly of addressable low-size domains of aggregated channels adapting their structure to external matrix environments, toward the construction of macroscopic films in which domains of percolated channels might exist.

AWCs with hydrophilic pores

According to the central pore structural features, AWCs can be mainly classified into two categories: AWCs with hydrophilic or hydrophobic pores. In this section, we review the hydrophilic AWCs, referring to the bottom-up supramolecular approach towards transmembrane biomimetic AQPs architectures.[21] Back in 2011, our group discovered the Imidazole-quartet (I-quartet) channels, resulting from the self-assembly of alkylureido-imidazoles **HC6H** or **HC6–8**, mutually stabilized by the scaffolding urea and imidazole–water hydrogen-bonding (Figure 4 a–f).[13] I-quartet water channels with 2.6 Å pores are dimensionally similar to AQPs channels. They form oriented dipolar water wires inside the tubular I-quartet architectures.[16] The inner water wires form through hydrogen-bonding with the channel wall and with vicinal waters, reminiscent of the encapsulated waters in AQPs. It is important to note that I-quartets are easily crystallized from ethanolic aqueous solutions, by selectively encapsulating only water molecules, even in the presence of salt solutes of other water mimics like sugars or glycerol. Based on these specific recognition effects, the I-quartets entirely exclude the incorporation of hydrated ions, favoring the transport water and H^+.

Water/proton transport activities of I-quartets through bilayer membranes decrease substantially with the decreasing length of the grafted alkyl chain: **HC8** ⩾ **HC6** > **HC4** (Figure 4 g, h).[16] Indeed, the tail length of octyl chains seems to be optimal. The increased permeability of the I-quartets is the result of their hydrophobic stabilization, based on the optimal interaction of the hydrophobic tails with the bilayer membrane.

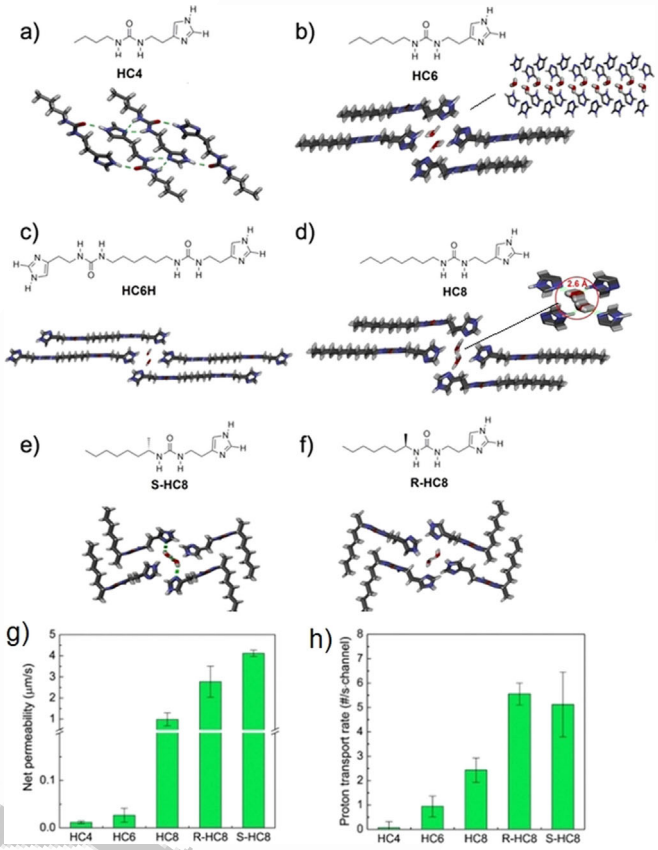

Figure 4. Top views of the I-quartet channels observed in their X-ray single-crystal structures of a) **HC4**, b) **HC6** (detail of the side view of the channel), c) **HC6H**, d) **HC8** (detail of the top-view of the channel), e) **S-HC8**, and f) **R-HC8**. g) Water permeabilities and h) proton conducting rates of I-quartet channels. Adapted with permission from reference [16a], copyright © 2016, American Chemical Society.

Molecular modelling studies show that permeation of water by I-quartet-by-I-quartet jumps is not linear in time, with intermediate steady states, between dynamic translational states on the timescale of ns (Figure 5 a).[22]

The computed patterns for chiral **R-HC8** and **S-HC8** channels have similar hydrogen-bonding patterns with 1.4–1.6 water–water hydrogen-bonds and 1.6–1.8 hydrogen-bonds linking waters to the imidazoles. With only 0.9 hydrogen-bonds, the water–water cohesion is lower for **HC8**. The total number of hydrogen-bonds for the waters reaches up to 3.2–3.4 hydrogen-bonds, very similar to a value of 3.2 hydrogen-bonds observed for bulk water.

The hydrogen-bonds in I-quartets exhibit a strong and constant stabilization of the water molecules of almost 20 kJ mol^{-1} for **S-HC8** or 13 kJ mol^{-1} for **R-HC8**. (Figure 5 b).[23] As a consequence, the water–water and water–channel interactions are both important to stabilize self-protecting selective water superstructures within the channels. The friction related to hydrogen-bonding events is not much stronger than that observed for bulk liquid water and, once stabilized within the channel, these structures do not need supplementary energy to translocate through the whole length of the channels. Ion transport through the bilayers incorporating the I-quartets was

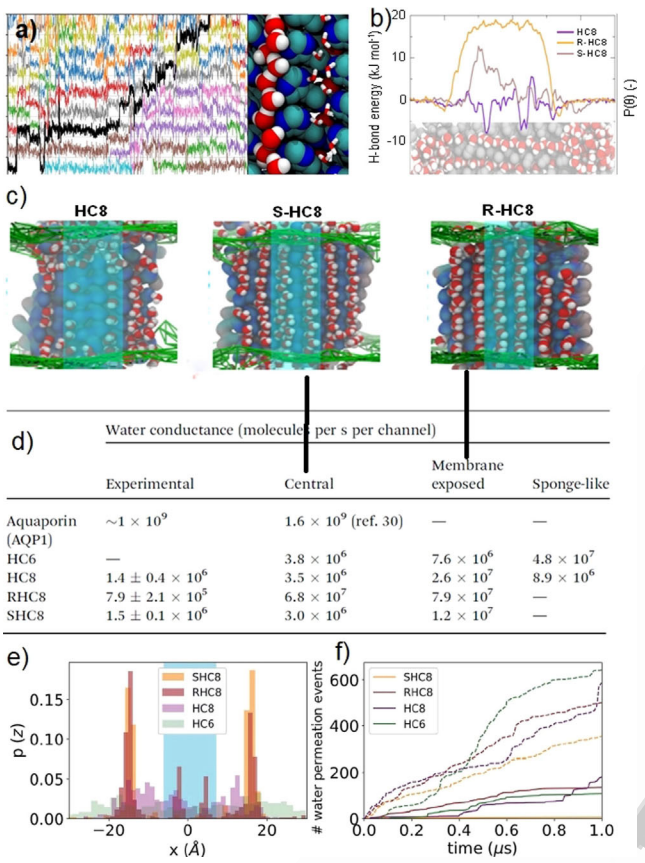

Figure 5. a) Dynamics of single water wires within I-quartet **RHC8**. The *z* axis position of water molecules versus time are displayed with different colors in individual channels.[22] b) Hydrogen-bond energy depicting the stabilization of waters within the two central water channels relative to bulk water.[23] c) MD simulations emphasizing the well-structured water wires in central channels and less structured sponge-like clusters of lateral membrane exposed channels. d) Experimental and simulated water conductance of central water wire channels or of lateral sponge-like channels. e) Water permeation in the crystal patch: the cyan region emphasizes the central water channels, protected from the lipids, whereas the white background displays membrane exposed lateral channels. f) Total transport of water molecules in both central pores shown as plain lines and lateral channel indicated as dashed lines, outward and inward directions across the membrane.[22] Adapted with permission from reference [22], copyright © 2018, Royal Society of Chemistry and from reference [23], copyright © 2016, American Association for Advancement of Science.

assessed by using HPTS (8-hydroxy-1,3,6-pyrene trisulfonate) fluorescence assays. No response versus the control experiment in the absence of the channels and no variation of the transport activity with variable concentration of I-quartets was observed. The reflection coefficient for NaCl, calculated as the ratio of the permeabilities in the presence of NaCl to that of sucrose osmolytes, ($113 \pm 15\,\%$, $n = 4$) indicates that the I-quartet channel achieve almost total salt rejection in a bilayer membrane.[16]

The I-quartets show an experimental water permeation rate of $1.4 \times 10^6\ H_2O\,s^{-1}\,channel^{-1}$, determined in bilayer membranes with a hydrophobic thickness of 3.5 nm and using 200 mM NaCl (8.3 bar) as the draw solution. From the single-crystal structures,[16] the density of I-quartet channels is 3.3×10^{17} channels m^2, which multiplied with $1.4 \times 10^6\ H_2O\,s^{-1}\,channel^{-1} = 4.6 \times 10^{23}\ H_2O\,s^{-1}\,m^{-2} = 49.2\ L\,m^{-2}\,h^{-1}$. Given an osmotic pressure of 8.3 bar (200 mM NaCl), the permeability of water through a 3.5 nm bilayer membrane is $P = 5.92\ L\,m^{-2}\,h^{-1}\,bar^{-1}$. Molecular modelling simulations have been performed on four I-quartet channels embedded within a bilayer membrane for water permeation (Figure 5c). The inspection of the I-quartets at the end of the MS shows that lateral channels tend to form a sponge-like, slightly disordered hydrogen-bonded water network, whereas the central channels remain very close to the water wires organization initially observed in the single-crystal structure. Water permeation prominently occurs at the most exposed membrane lateral positions, corresponding to slightly disorganized sponge-like structures. Compared with experimental single-channel permeances (Figure 5d–f), MS values have the same magnitude for central channels ($3 \times 10^6\ H_2O\,s^{-1}\,channel^{-1}$) with the exception of **RHC8** ($6.8 \times 10^7\ H_2O\,s^{-1}\,channel^{-1}$), which features a one order of magnitude higher permeation rate.[22] The sponge-like membrane exposed lateral channels that display higher conductance ($2.6–7.9 \times 10^7\ H_2O\,s^{-1}\,channel^{-1}$). Following the previously calculation, the sponge-like structures will allow a permeability of $P = 334\ L\,m^{-2}\,h^{-1}\,bar^{-1}$ through a 3.5 nm bilayer membrane for a osmotic pressure of 8.3 bar (200 mM NaCl), which is almost two orders of magnitude higher than the permeability of crystal water wires superstructures ($P = 5.92\ L\,m^{-2}\,h^{-1}\,bar^{-1}$). These values are superior to those observed for BWRO membranes ($2–8\ L\,m^{-2}\,h^{-1}\,bar^{-1}$),[8■■ok?■■] which are usually operated at slightly higher pressure (15–18 bars) and higher saline concentrations.

These experimental and theoretical studies are of tremendous importance as they show the adaptive behavior of water inside the channels depending on the environmental conditions, for which the structures of supramolecular self-assembled water are well defined. This reveals the stable selective water translocation pathways on the microsecond timescale; they can form water wires and sponges, which are still ion selective and more permeable. This discovery opens up new avenues in AWCs research, towards the construction of selective membranes for desalination.[24]

Although these I-quartet channels may be considered as highly water-permeable in bilayer membranes, they might behave differently when embedded in glassy polymeric membranes. Although single-crystal structures and MS simulations provide interesting information about their bilayer organization,[16,22,23] a detailed investigation must be reserved for further experimental work to construct highly selective polymeric membranes for desalination.

In 2014, our group reported a simple artificial T-channel, formed by self-assembly of bola-amphiphilic triazoles, mimicking the natural Gramicidin-A (gA) functions (Figure 6).[17] Water/proton permeability with large open channel conductance states and cation versus anion selectivity of the T-channel were revealed by molecular simulations and conduction assays. The water transport rate obtained for the T-channel ($k = 6.0 \times 10^{-4}\,min^{-1}$) is fifty times greater than the blank experiment ($k = 1.3 \times 10^{-5}\,min^{-1}$). Similar to gA, the cation transport activity sequence of the T-channel is $Li^+ < Na^+ < K^+ < Rb^+ \ll Cs^+$, and

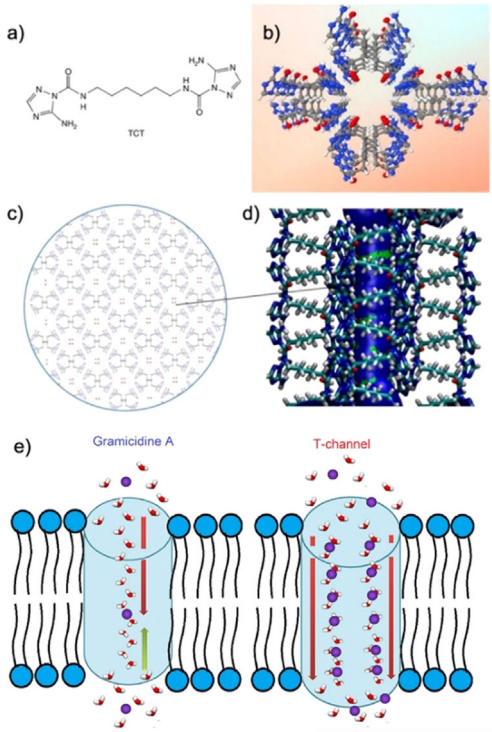

Figure 6. a) Chemical formula of bola-amphiphilic triazole **TCT**. b) Crystal structures of the T-channel. c) Top and d) side view in ball and stick representations of the T-channel. e) Single channel or multi-channel water/ion translocation through Gramicidin A and T-channels, respectively. Adapted with permission from reference [17c], copyright © 2014, Nature, Springer.

the Na^+ transport activity ($k = 2.7 \times 10^{-3}\,min^{-1}$) is two orders of magnitude higher than that of the Cl^- transport rate. Different from the cation-water single wire within the gA channel, the conductance of ions along the T-channel is surrounded by double file dipolar water wires, which might also inspire novel strategies for ion conducting processes.

Aquafoldamers are hydrogen-bonding-induced, helically folded aromatic molecules, which possess a channel interior containing pyridine N- and amide N-H-atoms, as hydrogen-bond acceptors and donors for water recognition. The helically folded aquapentamer (Figure 7a) accommodates solvent or water molecules in a tubular architecture with the size of approximately 2.8 Å, similar to the narrowest pore of AQPs. In 2012, Zeng et al. introduced the "sticky ends" strategy to electrostatically connect the helical two ends of short oligomers, which complementarily pile up and overlap to form one-dimensional helices embedding H_2O, MeOH, and CH_2Cl_2 (Figure 7b).[25a] Importantly, oriented water wires self-assemble within the pores of the helical stacks, which are first found to effectively transport protons with an efficiency comparable to that of Gramicidin A (Figure 7c).[25b] These results highlight the important role played by proton gradients, producing dynamic osmotic gradients, acting to synergistically facilitate the transport of confined water wires through the membrane. A series of crystallographic structures of aquafoldamers demonstrated a preferential recognition of the water versus methanol with a selectivity of about 17.7.[25c] Importantly, the approximately

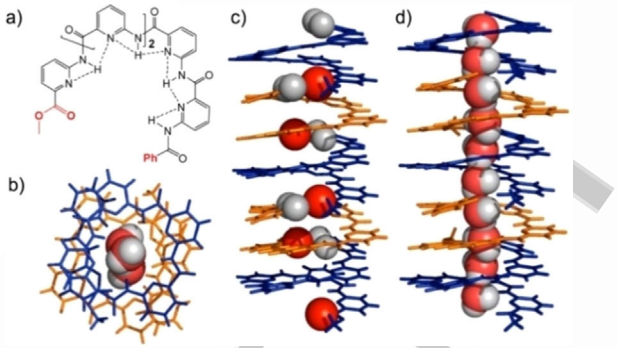

Figure 7. a) Chemical formula of aquafoldamer. b) Top view and c) side view of chiral helical stacks of the same handedness and d) adapted aquapores with high water permselectivity. Adapted with permission from reference [25c,d], copyright © 2014, 2020 American Chemical Society.

20% enlargement in Å-scale pore volume results in the formation of dynamic, more fluidic pores, which induce a 15-fold enhancement of water transport. This sheds light on the fastest AWC to date, which is able to translocate water at a rate of $\sim 3 \times 10^9$ $H_2O\,s^{-1}\,channel^{-1}$ with a high rejection of NaCl and KCl.[25d]

As for sponge-like I-quartet channels, a relaxed structure of the aquafoldamers, preserves the continual structure of water and induces higher and controlled diffusion of water inside the pore. The optimal deviation from the thermodynamically stable single-crystal structures is one of the most important features of synthetic water channels, synergistically improving water permeability and selectivity. The tedious synthetic route and relatively low general synthetic yield of the aquafoldamers limit their large-scale production. Their cylindrical shape would cause the functional channels to be oriented within the membrane scaffold, which would not constitute an insurmountable problem.

AWCs with hydrophobic pores

Inspired by the structure of the AQPs, hydrophobic NPA motifs allowing rapid permeation of water in the form of hydrogen-bonded single-file chains of water have been developed.[26] We present in the following part a few examples of biomimetic hydrophobic AWCs that serve the purpose of fast water conduction.

Carbon nanotube porins

Faster water transport through hydrophobic carbon nanotubes (CNTs) seems to be counter-intuitive at first when compared with the structure of natural AQPs (Figure 8). Over the past 20 years, extensive investigations have confirmed that water fills the CNTs interiors,[27] and ultrafast flow of water has been reported,[28] following the predictions from simulations.[29] Water weakly interacts with the hydrophobic walls, which contributes to its nearly frictionless transport, whereas the selectivity may be sterically controlled.[30] Ultrashort carbon nanotube porins (CNTPs)[32] have been successfully embedded in lipid bi-

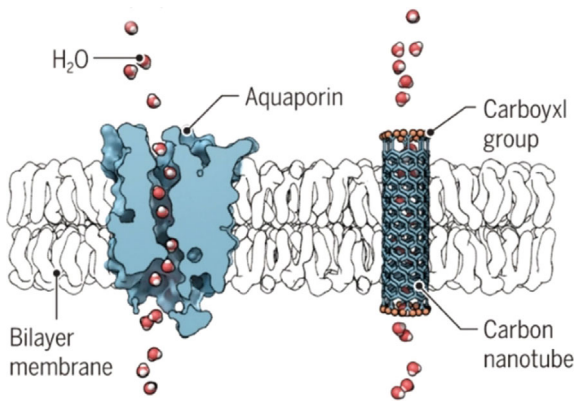

Figure 8. Schematic analogy between AQP and CNTs in lipid bilayers for the fast transport of water.[31] Adapted with permission from reference [31], copyright © 2017, National Academy of Sciences USA.

layers by Noy et al. and they demonstrate ultrafast proton permeability under nanoconfinement in CNTPs.[33] Later, the same group reported that narrow nCNTPs (6.8 Å diameter) transport 2.3×10^{10} $H_2O\,s^{-1}\,channel^{-1}$ (6.8×10^{-13} $cm^3\,s^{-1}$), whereas wide wCNTPs (13.5 Å diameter) had a single channel water permeability of 1.9×10^{9} $H_2O\,s^{-1}\,channel^{-1}$ (5.9×10^{-14} $cm^3\,s^{-1}$).[34] This is the first and a unique example of AWCs exceeding the water permeability of AQPs with osmotic pressure. Unfortunately, this incredible water transport rate, unlike AQPs, is not supported by their efficiency, as CNTPs were still able to transport ions. Reverse potential measurements revealed that the nCNTPs had a P_{K^+}/P_{Cl^-} selectivity of 184 at seawater salinity level, indicative of possible desalination applications. Later, Freger estimated the water salt permselectivity of nCNTPs to be 10^4, one order of magnitude lower than the target set for the desalination membranes.[35]

Dendritic dipeptides

Percec et al. reported synthetic dendritic dipeptides that are able to self-assemble through multivalent hydrogen-bonding into helical porins with an inner pore of 12.8 ± 1.2 Å.[36a] Their conformation is controlled by the solvent and the dendrons were found to be able to assemble as hydrophobic pores for proton translocation through a Grotthuss mechanism, for which water must mediate the proton migration.[37] Three years later, water transport driven by osmotic pressure through more stable pores assembled from modified dendrons was directly observed by the same group, making this the first example of AWCS in bilayer membranes (Figure 9).[36b] Additionally, multinuclear NMR studies showed no transport of monovalent ions Li^+, Na^+, and Cl^-. However, there is no elucidation of the mechanism for the selective exclusion of these monovalent ions by the 14 Å pores.

Shape-persistent macrocyclic channels

A series of hexa(*m*-phenylene-ethynylene) ***m*-PE** macrocycles were synthesized by Gong et al.[38] with the aim of developing

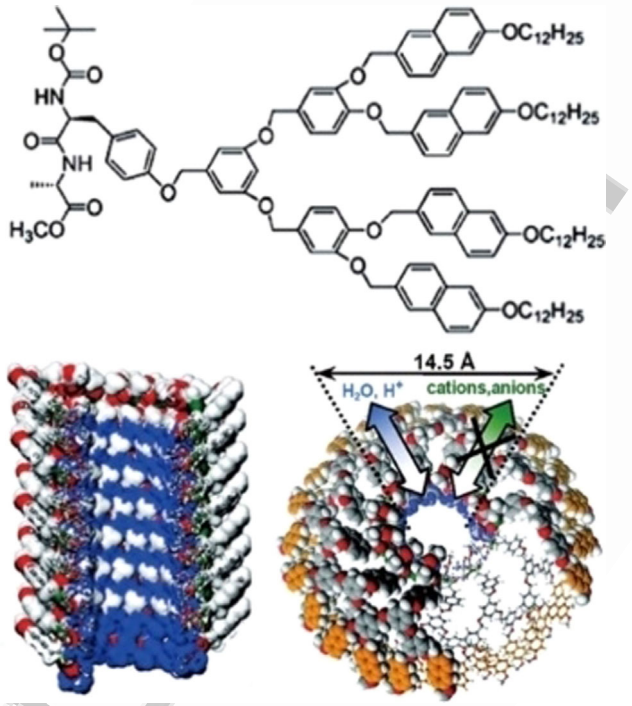

Figure 9. Chemical structure of dendritic dipeptide and the side and top views of their self-assembled helical tubular porins.[37] Adapted with permission from reference [37], copyright © 2007, American Chemical Society.

well-defined synthetic self-assembled nanopores, thanks to the multiple hydrogen-bonding and π–π stacking interactions between the side chains (Figure 10).

The helical stacked macrocycle has a defined pore with an internal van der Waals diameter of 6.4 Å. Direct measurement of water transport by stopped-flow assays demonstrated faster net flow of water across the lipid bilayer under osmotic stress, with an estimated water permeability of 4.9×10^7 $H_2O\,s^{-1}\,channel^{-1}$, representing about 20% that of AQP1. Besides that, the single-channel conductance exhibited a remarkable P_{H^+}/P_{Cl^-} selectivity of over 3000. A significant lower permeability for K^+ compared with H^+ is also inferred. These self-assembled synthetically accessible, robust nanostructures

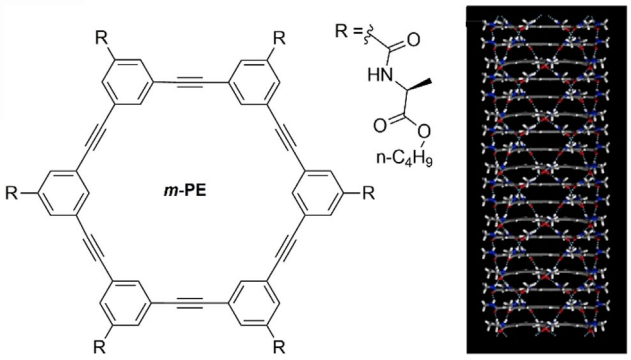

Figure 10. Molecular structure of *m*-oligophenylethynyl ***m*-PE** macrocycles and the helical stack of the macrocycles demonstrated from the simulation.[23] Adapted with permission from reference [38], copyright ©2012, Nature Springer.

are good alternatives to hydrophobic pores such as CNTs and pillar[5]arenes.[39]

Hydrazide-appended pillar[5]arene

First introduced in 2008, by Ogoshi et al.,[40] pillararenes represent an interesting class of symmetrical synthetic hosts with electron-rich interiors, variable size, and versatile functionality of their cavity.[41]

The formation of single-crystal nanotubes of pillar[5]arene (PA[5]) under the template effect of water wires[42] inspired the pioneering work by Hou and his group in which several AWCs based on PA[5] were developed.[43] By connecting two PA[5] with an suitable aliphatic arm, they created a H^+ channel with higher permeability than the original monomers (Figure 11).[43b] The isotope effect shows that the proton transport proceeded through the Grotthuss mechanism.[37] Functional hydrazide PAH[5] derivatives were then synthesized. Their tubular structures form through intramolecular hydrogen-bonding of the hydrazide subunits. The single-crystal structure of the shortest PAH[5] derivative revealed that the water was absent in the hydrophobic region, resulting in encapsulated water dimers within the hydrazide side chain rather than water wires.[43b] Their permeability was estimated to be 8.6×10^{-10} cm s^{-1} or 40 H_2O s^{-1} channel^{-1}. The PAH[5] showed no proton transport, yet clear hydroxide transport was monitored by HPTS assay, corroborating the presence of truncated water wires in the crystal structures. Together with I-quartet channels, the hydrazide PAH[5] channels are the first examples of synthetic molecules mimicking the water transport function of AQP, while rejecting all ions/no protons (I-quartet) or only proton/no ions (PAH[5]). No other channels before these systems have been considered as artificial AQPs. They are pioneering in the field and despite their lower permeability, they still represent unique examples with interesting selectivity compared with other novel, more permeable, but non-selective AWCs more recently developed.

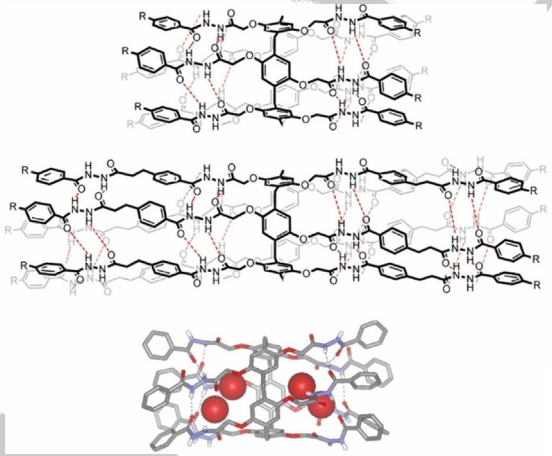

Figure 11. Chemical structures of hydrazide-attached pillar[5]arene monomolecular channels, and single-crystal structure of the shorter pillar[5]arene counterpart.[43b] Adapted with permission from reference [43b], copyright © 2012, American Chemical Society.

Peptide-appended pillar[5]arene

Hou et al.[45] later developed a second-generation pillararene PAP[5] with unimolecular channels, first used for the selective transmembrane transport of chiral amino acids. Instead of hydrazide, the authors appended hydrophobic phenylalanine side chains to improve their insertion rate (Figure 12a). The change resulted in a distinct boost in performance within two orders of magnitude to the permeability of AQP1, as the water permeability reaches 1.0×10^{-14} cm^3 s^{-1} (3.5×10^8 H_2O s^{-1}) as determined by stopped-flow light-scattering measurements in cooperation with Kumar group. Interestingly, hexagonal supramolecular arrays of PAP[5] can be easily packed in lipid bilayers on samples of 100 nm scale. Molecular simulations show that partial (80%) permeation events can be detected through water-filled PAP[5] channels, whereas the remaining 20% of them were devoid of water or were blocked by lateral phenylalanine chains, present within the pillararene core. Moreover, the PAP[5] (4.7 Å) cannot reject ions and showed the cation selectivity follows the trend: $NH_4^+ > Cs^+ > Rb^+ > K^+ > Na^+ > Li^+ > Cl^-$. The molecular cutoff of 420 Da of the PAP[5] channel is not suitable for selective removal of salts and other small molecules required by desalination.

A subsequent study by Kumar et al.[47] demonstrated the successful PAP[5] incorporation into block-copolymer membranes with a substantial increase of pore (channel) packing density of approximately 4.2×10^5 μm^{-2} (determined again at nm scale films), which are a few orders of magnitude higher than CNTs packing or than polymeric iso-porous membranes. Micrometric PAP[5]/polybutadiene-polyethylene-oxide 2D

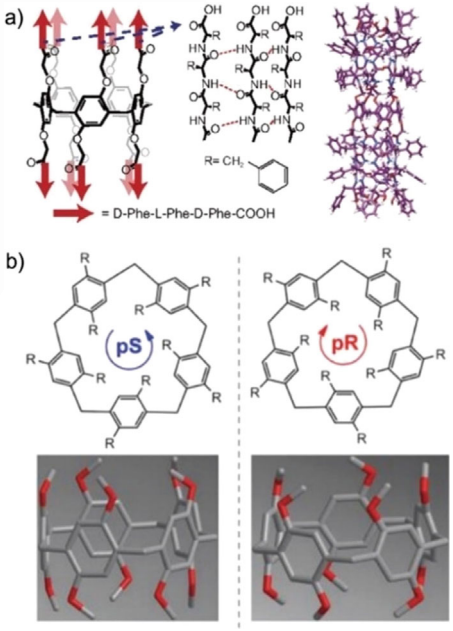

Figure 12. a) Chemical structure and molecular modeling representation of the Phe_3-pillar[5]arene PAP[5] channel.[46] b) The chiral pS and pR-isomers of PAP[5] pillar[5]arene.[48] Adapted with permission from reference [46], Copyright © 2015, National Academy of Sciences USA. Adapted with permission from reference [48], copyright © 2019, Wiley.

sheets have been prepared and stacked by polyelectrolyte PEI insertion. The bioinspired composite membranes displayed an over 10-fold permeability ($\approx$65 L m^{-2} h^{-1} bar^{-1}) enhancement over other commercial membranes (4–7 L m^{-2} h^{-1} bar^{-1}) and a sharp, selective molecular weight cutoff of $\approx$500 Da. Although PAP[5] channels showed a ion selectivity K^+/Cl^- ratio of 10, and a permselectivity of 0.83, similar to CNTs channels,[34] high NaCl rejection cannot be observed at the macroscopic level of membranes during hydraulic pressure assisted filtration tests. This difference is indicative of the very difficult challenges in translating the molecular transport properties of single channels to macroscopic materials with a similar filtration performance. A better nano-distribution of channels and physical and chemical mismatch with the material matrix may allow the perfect membrane homogeneity to be reached.

Wang and co-workers[48] prepared a structurally similar PAP[5], and isolated two diastereomers, namely pS and pR-PH (Figure 12b). Although pR-PH had a single-channel water permeability of 3.9×10^{-14} cm^3 s^{-1}, its isomer displayed no water transport activity. Molecular simulations show that the PheAla side chain of pS-PH blocks the channel in contrast to a well-maintained open channel state for pR-PH, through which water permeates in single-file fashion. In addition, the authors prepared a supported lipid membrane with the incorporation of the pR-PH channels, which had improved LPRO performance in terms of both water nanofiltration flux ($\approx$30 L m^{-2} h^{-1} bar^{-1} compared with $\approx$17 L m^{-2} h^{-1} bar^{-1} of the control membrane) with a low salt rejection of $\approx$88% Na_2SO_4, although NaCl rejection is not reported.

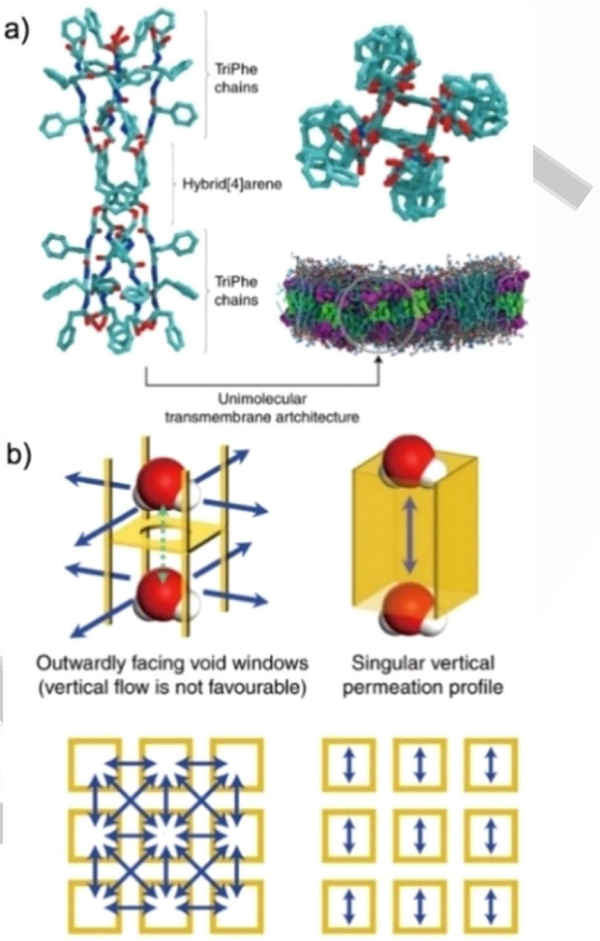

Figure 13. a) Molecular model of the peptide-pillar[4]arene, PAH[4]. b) Proposed water permeation conduits (blue arrows) between PAH[4] (left) and traditional AWC (right) configuration.[49] Adapted with permission from reference [49], copyright © 2020, Nature, Springer.

Peptide-appended hybrid[4]arene

To optimize the water/salt selectivity of the AWCs, novel synthetic channels with pore sizes smaller than PAP[5] ($\approx$4.7 Å) have been developed. Hou and Kumar[49] have reported a new four-membered pillararene PAH[4] by grafting eight D-L-D-PheAla tripeptides to construct a pore of $\approx$3 Å, an optimal pore size for selective water permeation (Figure 13). Quantitative measurements have shown that 3.7×10^9 water molecules pass through PAH[4] every second (or1.1×10^{-13} cm^3 s^{-1} channel^{-1}) at 25 °C, which is comparable to the value of AQP1. The exceptionally high water permeability becomes apparent especially when the density of the channel reaches the threshold between 20 to 45 channels per vesicle. Indeed, molecular dynamics (MD) simulations reveal that PAH[4] assembles into the lipid membrane, but, unlike PAP[5], it does not provide a straightforward inner pathway for water molecules. The cooperative water-permeating pathways were formed between the PAH[4] molecules, giving insights into the water permeation through cluster-forming AWCs. An energy barrier as low as 3.6 kcal mol^{-1} for the water permeation was observed for PAH[4] when using PEG osmolyte, indicative of single-file water transport. This impressive result confirms that enhanced water permeability can be observed and is confirmed when water cluster-forming organic nanoarchitectures self-assemble in lipid membranes. I-quartet sponge channels[22,24] or porous organic cages (POCs)[50] have been previously described in 2018 and 2019, which feature the rather unique enhanced permeability of water clustering conduction systems.

A significantly low Cl^- permeability of 9.5×10^{-23} cm^3 s^{-1} was determined by using a low concentration salt osmolyte, which helps PAH[4] to achieve a $\approx10^9$ water/salt selectivity in bilayer membranes, far beyond the requirements for desalination membranes by at least four orders of magnitude.

However, it is worth mentioning that a few obstacles need to be overcome first to realize the projected performance of PAH[4] in bilayer membranes toward macroscopic membranes for RO desalination at high pressure. Nevertheless, the concept of engineering transient cluster/sponge membrane water channels is clearly evolving, as it considerably expands the range of possibilities for the specific design of macroscopic RO membrane materials embedding AWCs.[24,51]

We very recently discovered that modification of the rims of pillar[5]arene (5 Å diameter) may led to the narrowest constriction pores of 2.6–2.8 Å diameter within the same structure (Figure 14),[52] similar to the selective hourglass structure of AQPs.[6] This affords control of the translocation by size restric-

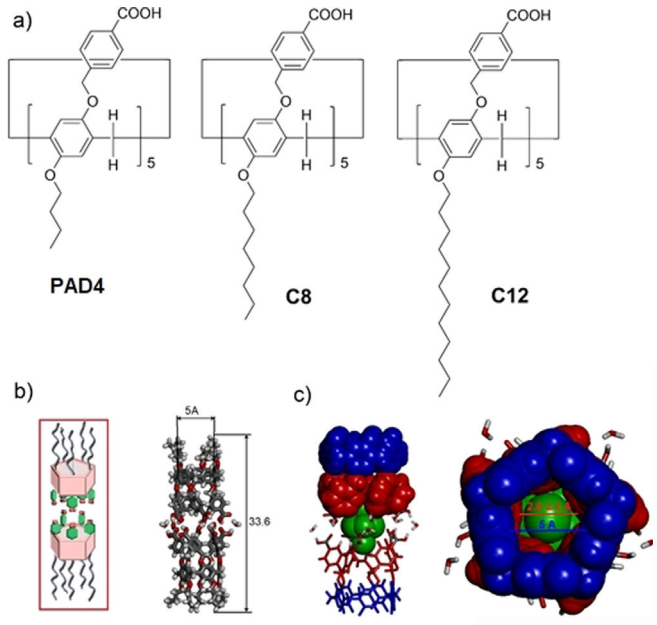

Figure 14. a) Structures of peralkylcarboxylate-pillar[5]arenes PAD4, PAD8, and PAD12. b) Crystalline solid-state structure showing the dimeric channel structure of 34 Å length and c) a variable pore geometry composed of pillar[5]arene (blue) of 5 Å diameter and of the narrowest twisted carboxyphenyl pore of 2.8 Å diameter (red).

tion along the resulting PAD channels at the selectivity filter level. The water permeability of $\approx 10^7$ water molecules s^{-1} channel^{-1} is only one order of magnitude lower than that of AQPs and importantly they reject alkali cations. Different to I-quartets where, during their translocation, the water molecules interact along the whole structure of the channel, for the PAD channels, their interactions are mainly related to the narrowest pore structure, which is large enough for the water molecules to pass, but restrictive enough to block the passage of hydrated Na^+ or K^+ cations.

Biomimetic AWC Membranes for Desalination

The AWCs optimized in terms of high permeability and ion rejection in bilayer membranes would be naturally used as active components for the preparation of biomimetic membranes for desalination. The next important steps are related to maintaining the channel activity observed at the single-channel level in bilayer membranes and to obtain a high channel density on the surface of the membrane support. The major challenge relates to the strategy used for scaling-up functional high-density membranes of meter-scale filtration surface areas.

Several ideal designs may be proposed for producing membranes, including AWCs physically included in thin-layer polymers or the chemical synthesis of polymers from AWC monomers suspended as thin layers over planar or hollow fiber supports (Figure 15a). An interesting alternative is to generate polymeric cross-linked networks from AWC monomers, further cast on support membranes (Figure 15b).

One clear advantage is that the AWCs may be more readily stabilized than AQPs in the membrane structures. In other

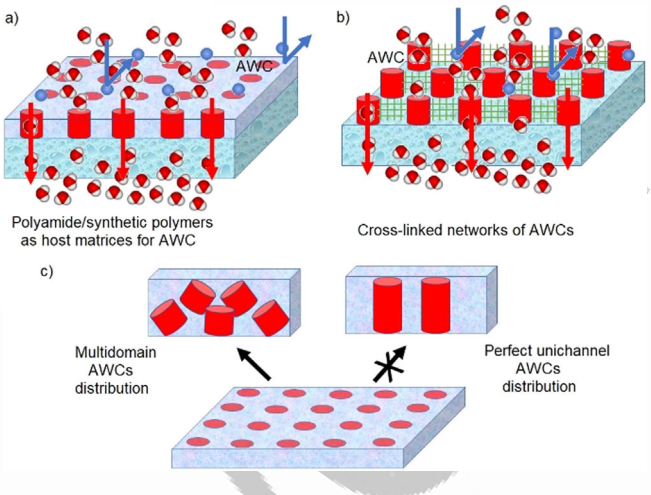

Figure 15. Direct inclusion of AWCs in biomimetic membrane supported thin layers. a) Polyamide or polymeric host matrices for AWCs or cross-linked networks of AWCs for scalable membranes. Translocation/high salt ejection governed by water–ion interactions within selective AWC superstructures. c) Multi-domain versus uni-channel distribution of AWCs at the nanometric scale within macroscopic thin-layer membrane materials.

words, one might expect the use of AWCs to lead to the formation of highly permeable layers with excellent salt rejection.

We already have the experience for upscaling the supramolecular channels to macroscopic membranes.[53] Accordingly, several synthetic routes have been reported and it is impossible to achieve a perfect channel alignment from one side to the other side of the active layer without using a directional scaffolding matrix (Figure 15c). Multidomain AWCs distributed with different orientations can be "frozen" in a macroscopic matrix at the nanometric level by compacting directional columnar self-assembled channels, as a straightforward upscaling approach to high-performance, next-generation, thin-layer membranes for desalination.[54]

The desalination performances of AWCs are mostly related to important challenges in translating the transport properties of the molecular self-assembled channels to performant meter-scale membrane materials and filtration modules needed for desalination. We postulated that one of the creative strategies for addressing the scale-up challenges is to combine the thin-film composite TFC polyamide membrane, known for its scalability by integration within a typical roll-to-roll processing system with the highly permeable and selective AWCs. An easy strategy is to directly incorporate dense networks of AWCs while forming the selective layer of the membrane. Polyamide layers already used for RO filtration are highly desired as the mechanically stable matrix to support the AWCs.

Thin-film composite membranes (TFCs) are currently implemented in the water desalination industry and around 90% of used membranes are based on RO/NF technologies.[8] In the early steps, interfacial polymerization (IP) was used to form a TFC thin layer on the support, but this method was not used in industrial fabrication until Cadotte[55] proposed polyamide (PA) composite membranes with an interestingly high flux, which could be prepared by interfacial polymerization of amines and acylchlorides and with varying performances that

can be easily reproduced on the laboratory and industrial scales.

With the development of nanomaterials, thin-film nanocomposites (TFNs) have been prepared by the physical inclusion of solid nanocrystals into the polyamide layer of a TFC membrane. Several types of zeolites, metal–organic frameworks (MOFs) or cellulose nanocrystals have been used to obtain TFNs.[8] By using a modified strategy, distinct nanocrystalline sponge I-quartet AWCs have been incorporated into the polyamide layer (Figure 16a). A typical AWCs incorporation experiment to obtain nanocrystals uniformly disposed in a PA layer includes the injection of a colloidal solution of the I-quartets in a water-miscible solvent on the top of the membrane. The diffusion of organic solvent into the water causes the AWCs to crystalize and to be incorporated within the PA network during the IP process as shown by SEM images of the reference (Figure 16b) and hybrid (Figure 16c,d) membranes. To optimize the incorporation, the defect control has been achieved by varying the nature and the concentration of the PA monomers to ensure readiness for the membrane fabrication process. Such uniform distributed nanocrystals of AWCs have been in situ generated from a soft colloidal solution, which forms solid particles during the IP process. This induces a gentle adaptive generation of densely packed AWCs homogeneously integrated within a PA matrix, which allowed us to identify new membranes that remarkably outperform the control TFC polyamide RO membranes in the treatment of saline feed SWRO streams. The AWC-RO biomimetic membrane of 70 cm^2 provides 99.5–99.8% rejection of NaCl with a water flux of 75 $L\,m^{-2}\,h^{-1}$ or 2.8 $LMH\,bar^{-1}$ (+200% larger than a commercial TFC membrane) at 65 bar applied pressure with 35000 ppm feed solution for seawater desalination. This is more than 75% higher than the flux with equivalent solute rejection and a noteworthy 12% reduction of the required energy compared with the application of current approaches of commercial membranes for desalination.

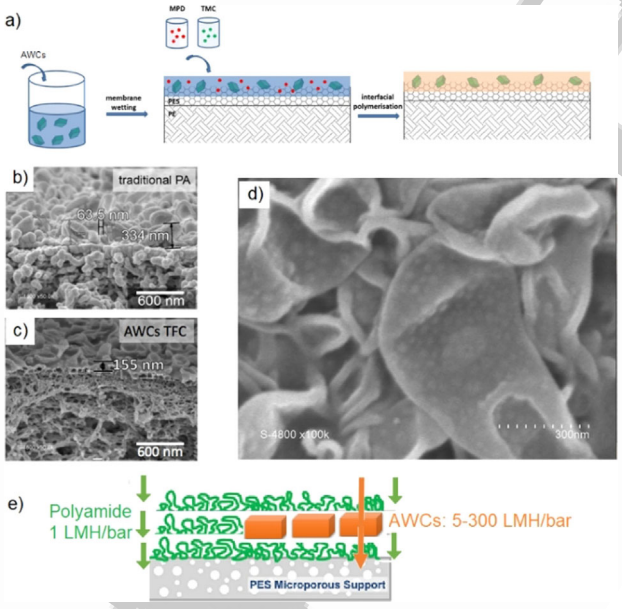

Figure 16. a) AWC-PA membrane fabrication with incorporated AWC nanoparticles of I-quartets in PA thin-layer membranes. Representative scanning electron microscopy (SEM) micrographs of b) the top view of the surface of a traditional TFC membrane, c) TFC polyamide with AWCs, and d) cross-sectional view of the uppermost active layer including distributed AWCs—as the white dots of 30–40 nm, uniformly included in the PA layer. e) Composite PA-AWC layers with slow (PA) and very fast (AWC) permeating regions contributing to a higher permeation observed through hybrid AWC-PA membranes.

These initial studies on the inclusion of AWCs within the PA structure led to a greater fundamental understanding of how selective pores can be optimized at the nanoscale to facilitate ultrafast and highly selective transport of water, mainly occurring through selective channels, and to minimize the translocation of ions and molecules bypassing the membrane. The selective highly permeable AWCs will play the role of active and selective relays for which the water transport occurs at the nanometric level with higher permeability up to 300 $LMH\,bar^{-1}$ (see above) compared with the self-supportive PA membrane for which the permeability is 1 $LMH\,bar^{-1}$ (Figure 16e). The overall permeability of the hybrid AWC-PA membrane will be composed from slow (PA) and very fast (AWC) permeating regions, contributing to a higher overall permeation through nano-dispersed AWC-PA membranes.

Conclusions and Outlook

The first identification of AWCs by our group in 2011[13] opened the door to new fundamental and applicative research on AWCs similar to natural ones.[3,15,21] We speculated at this time that biomimetic AWCs might have important influences to increase the driving force of the transport by using natural paradigms and improve the water desalination performances. All these assumptions have been confirmed during the last decade.

AWCs present robust and functional structures (2011), which selectively conduct water through bilayer membranes (2014) and could support better scale-up and mechanical requirements (2016), which seem to not impair the re-structuring of AQP biomimetic membranes (2018; Figure 17). Learning from the complex structures of biological channel proteins is an important endeavor (2018). Different scientific advances including novel experimental and modeling experiments complement each other for a more complete understanding of water structuration and mechanisms to translocate water in biological pathways (2018).

Straightforward easy preparation of AWCs—artificial AQPs—give rise to novel strategies towards the design of highly selective membranes that transport water with unprecedented fluxes (2019). The next step is related to up-scaling membrane and related filtration processes.

Owing to the notable simplest structural features of AWCs, for instance, most of them are low cost and synthetically accessible with chemical robustness, they have been identified as promising alternatives to AQPs. Over the past decade, the increase of relevant publications in this field clearly indicates that the design and functionalization of various AWCs offers

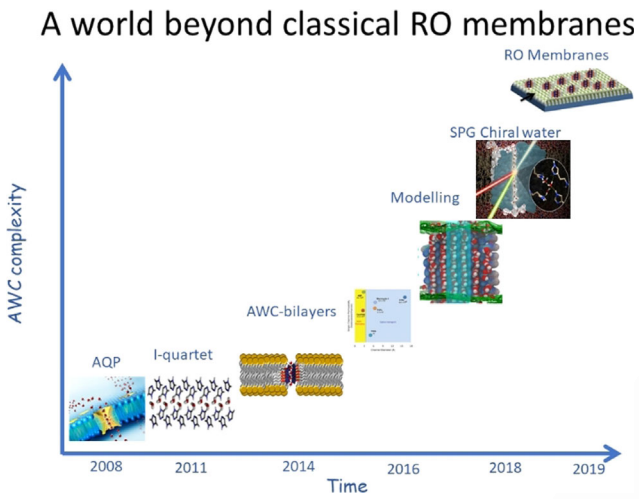

Figure 17. AWC development with time towards highly competitive RO membranes for desalination.

flexible avenues toward mimicking natural AQPs in bilayer membranes (Table 1).[23b]

Again, efforts to achieve both high selectivity and reasonable permeability is an important challenge for AWC channels. High permeability has been mostly achieved by designing tubular structures with inner hydrophobic pores for water translocation. During the last decade, the permeation trough such frictionless inner pores was increased by 2–4 orders of magnitude, reaching that of natural AQPs. The water-over-ions selectivity of such hydrophobic AWC systems can be achieved only with dimensionally limited pores ($d < 0.6$ nm). For larger AWCs porins, the rearrangements at the entry of the pore control the hydrogen-bonding of water patterns that further self-assemble with variable density in the available inner space of the porin.[34]

There is only the steric confinement that controls the supramolecular water recognition, whereas water self-clustering cannot totally avoid the ion permeation through AWCs, impeding their permselectivity. Several AWCs demonstrated a preferential recognition of water over ions or small molecules through specific hydrogen-bonding of water with a high selectivity factor near to perfect rejection.[14,25] The optimal binding of water in interaction with the recognition groups on the inner surface of the channel is an important prerequisite for its selection. Importantly, the deviation from the thermodynamically stable, hydrogen-bonded, strongly confined structures observed within the single-crystal structures toward more relaxed molecules of supramolecular aggregates, which generate more relaxed and highly permeable water clusters, is one of the most important discoveries that can be considered for the simultaneous improvement of both water permeability and selectivity. Relaxed I-quartet sponges, [22,24] aquafoldamers,[25d] or porous organic cages (POCs)[50] as well as confined pillararene networks are representative examples that have been independently reported during the last two years (2018–2020)!

The key structural features that enable efficient translocation of water are high permeation through hydrophobic channels for fast water translocation, whereas molecular recognition selectivity filters (SF) are the prerequisite for high selectivity. The AWCs reported to date use water binding sequences along the entire pore length, rather than only in a very specific selectivity filter region like natural porins for which the selection occurs only in the very short SF region.

Thus, AWCs, which are fundamental in nature, will allow us to develop new knowledge on the natural principles of selective water translocation and gain a greater understanding of the fabrication of highly competitive biomimetic membranes for desalination. The thin-layer polyamide membranes, used for water desalination since 1972, have improved dramatically over the last 60 years; however, their low-resolution structure and the transport mechanism are still poorly understood. The ultimate performance of a membrane is usually determined by an increased flux (or permeance) owing to the introduction of defects in the membrane structure lowering the selectivity, which is always decreasing.

Table 1. Overview of the features of current reported water channels.[23b]

Channel	Type of pore	Pore size	Water permeability/selectivity
AQPs[2]	hydrophilic	2.8 Å	4×10^9 waters s^{-1} channel^{-1}, high selectivity for water, rejects all ions and H^+
I-quartet[5–6,36]		2.6 Å	1.5×10^6 waters s^{-1} channel^{-1}, high selectivity for water, rejects all ions except H^+
T-channel[7]		≈2.5–4 Å	No water permeability reported, enhanced conduction states for alkali cations and protons
aquafoldamer[8]		≈2.8 Å	No water permeability reported, rejects all ions except protons
nCNTPs[17]	hydrophobic	6.8 Å	2.3×10^{10} waters s^{-1} channel^{-1}, rejection of ions only in dilute solutions
wCNTPs[17]		13.5 Å	1.9×10^9 water molecules s^{-1} channel, no selectivity for water
dendritic dipeptide[19–20]		12.8 ± 1.2 Å	No reported permeability, rejects ions except H^+; attributed to hydrophobic entrance effects
m-PE[23]		6.4 Å	4.9×10^7 water molecules s^{-1} channel^{-1}, no water selectivity, a remarkable P_{H^+}/P_{Cl^-} selectivity over 3000, and a significantly lower conduction for K^+ compared with protons
PAH[5][28]		4.7 Å	40 water molecules s^{-1} channel^{-1}, no selectivity for water, transports alkali cations but no conduction for protons
PAP[5][30]		4.7 Å	Swelling: 3.5×10^8 water molecules s^{-1} channel^{-1}; shrinking: 3.7×10^6 water molecules s^{-1} channel^{-1}, no selectivity for water, good activity for alkali cations
PAH[4][33]		≈3 Å × ≈5 Å	3.7×10^9 water molecules s^{-1} channel^{-1}, $\approx10^9$ water/salt selectivity

I-quartet: imidazole-quartet; nCNTPs: narrow carbon nanotube porins; wCNTPs: wide carbon nanotube porins; *m*-PE: hexa(*m*-phenylene ethynylene); HAP[5]: hydrazide-appended pillar[5]arene; PAP[5]: peptide-appended pillar[5]arene; PAH[4]: peptide-appended hybrid[4]arene.

The result of the fast and selective transport of water through the AWCs has enormous benefits for several practical applications: advanced desalination, production of ultrapure water for biomedical or electronic applications, purification of highly diluted solutions. We believe that AWCs have enormous potential to become an integral part of breakthrough water desalination and purification technologies. They will promote the fabrication of channel-based membranes for enhanced low-energy desalination, blue energy harvesting, production of ultrapure water for medicine and electronics, and purification of residual water.

We believe that AWCs will provide the right information at the right time by changing a 60-year-old desalination paradigm only a decade after they were discovered.

Acknowledgments

This work was supported by Agence Nationale de la Recherche ANR-18-CE06-0004-02, WATERCHANNELS, and by the Centre National de la Recherche Scientifique-Programme interdisciplinaire MITI -BIOMIMETISME.

Conflict of interest

The authors declare no conflict of interest.

Keywords: bilayer membranes · biomimetic · desalination · self-assembly · water channels

[1] J. Eliasson, *Nature* **2015**, *517*, 6 – 7.
[2] M. M. Mekonnen, A. Y. Hoekstra, *Science Adv.* **2016**, *2*, e1500323.
[3] M. Barboiu, A. Gilles, *Acc. Chem. Res.* **2013**, *46*, 2814 – 2823.
[4] a) P. Ball, *Chem. Rev.* **2008**, *108*, 74 – 108; b) P. Ball, *Proc. Natl. Acad. Sci. USA* **2017**, *114*, 13327 – 13335.
[5] a) K. Murata, K. Mitsuoka, T. Hirai, T. Walz, P. Agre, J. B. Heymann, A. Engel, Y. Fujiyoshi, *Nature* **2000**, *407*, 599 – 605; b) P. Pohl, S. M. Saparov, M. J. Borgnia, P. Agre, *Proc. Natl. Acad. Sci. USA* **2001**, *98*, 9624 – 9629; c) B. L. de Groot, H. Grubmuller, *Curr. Opin. Struct. Biol.* **2005**, *15*, 176 – 183.
[6] P. Agre, *Angew. Chem. Int. Ed.* **2004**, *43*, 4278 – 4290; *Angew. Chem.* **2004**, *116*, 4377 – 4390.
[7] a) E. Tajkhorshid, P. Nollert, M. O. Jensen, L. J. Miercke, J. O'Connell, R. M. Stroud, K. Schulten, *Science* **2002**, *296*, 525 – 530; b) A. Horner, C. Siligan, A. Cornean, P. Pohl, *Faraday Discuss.* **2018**, *209*, 55 – 65; c) U. Kosinska Eriksson, G. Fischer, R. Friemann, G. Enkavi, E. Tajkhorshid, R. Neutze, *Science* **2013**, *340*, 1346 – 1349; d) U. Zachariae, T. Kluhspies, S. De, H. Engelhart, K. Zeth, *J. Biol. Chem.* **2006**, *281*, 7413 – 7420; e) C. I. Lynch, S. Rao, M. S. P. Samsom, *Chem. Rev.* **2020**, *120*, 10298 – 10335.
[8] Z.-J. Yan, D. D. Wang, Z. J. Ye, T. Fan, G. Wu, L. Y. Deng, L. Yang, B. X. Li, J. W. Liu, T. H. Ma, C. Q. Dong, Z.-T. Li, L. H. Xiao, Y. F. Wang, W. N. Wang, J.-L. Hou, *J. Am. Chem. Soc.* **2020**, *142*, 15638 – 15643.
[9] a) C. Y. Tang, Y. Zhao, R. Wang, C. Hélix-Nielsen, A. G. Fane, *Desalination* **2013**, *308*, 34 – 40; b) C. Y. Tang, Z. Wang, I. Petrinić, A. G. Fane, C. Hélix-Nielsen, *Desalination* **2015**, *368*, 89 – 105; c) Z. Yang, X.-H. Ma, C. Y. Tang, *Desalination* **2018**, *434*, 37 – 59; d) Z. Yang, H. Guo, C. Y. Tang, *J. Membrane Sci.* **2019**, *590*, 117297; e) M. Kumar, M. Grzelakowski, J. Zilles, M. Clark, W. Meier, *Proc. Natl. Acad. Sci. USA* **2007**, *104*, 20719 – 20724.
[10] a) C. Hélix-Nielsen, *Membranes* **2018**, *8*, 44; b) Y. Lia, S. Qia, M. Tiana, W. Widjajantia, R. Wang, *Desalination* **2019**, *467*, 103 – 112; c) Y. Zhao, C. Qiu, X. Li, A. Vararattanavech, W. Shen, J. Torres, C. H. Nielsen, R. Wang, X. Hu, A. G. Fane, C. Y. Tang, *J. Membr. Sci.* **2012**, *423 – 424*, 422 – 428; d) Y. He, H. Hoi, S. Abraham, C. D. Montemagno, *J. Appl. Polym. Sci.* **2017**, *134*, 46169; e) X. Li, S. Chou, R. Wang, L. Shi, W. Fang, G. Chaitra, C. Y. Tang, J. Torres, X. Hu, A. G. Fane, *J. Membr. Sci.* **2015**, *494*, 68 – 77; f) Z. Li, R. Valladares Linares, S. Bucs, L. Fortunato, C. H. -Nielsen, J. S. Vrouwenvelder, N. Ghaffour, T. O. Leiknes, G. Amy, *Desalination* **2017**, *420*, 208 – 215.
[11] S. Hernández, C. Porter, X. Zhang, Y. Weib, D. Bhattacharyya, *RSC Adv.* **2017**, *7*, 56123 – 56136.
[12] a) Y.-M. Tu, W. Song, T. Ren, Y.-X. Shen, R. Chowdhury, P. Rajapaksha, T. E. Culp, L. Samineni, C. Lang, A. Thokkadam, D. Carson, Y. Dai, A. Mukthar, M. Zhang, A. Parshin, J. N. Sloand, S. H. Medina, M. Grzelakowski, D. Bhattacharya, W. A. Phillip, E. D. Gomez, R. J. Hickey, Y. Wei, M. Kumar, *Nat. Mater.* **2020**, *19*, 347 – 354; b) A. G. Livingston, Z. Jiang, *Nat. Mater.* **2020**, *19*, 257 – 258.
[13] Y. Le Duc, M. Michau, A. Gilles, V. Gence, Y. M. Legrand, A. van der Lee, S. Tingry, M. Barboiu, *Angew. Chem. Int. Ed.* **2011**, *50*, 11366 – 11372; *Angew. Chem.* **2011**, *123*, 11568 – 11574.
[14] a) M. Barboiu, *Angew. Chem. Int. Ed.* **2012**, *51*, 11674 – 11676; *Angew. Chem.* **2012**, *124*, 11842 – 11844; b) X. B. Hu, Z. Chen, G. Tang, J. L. Hou, Z. T. Li, *J. Am. Chem. Soc.* **2012**, *134*, 8384 – 8387.
[15] M. Barboiu, *Chem. Commun.* **2016**, *52*, 5657 – 5665.
[16] E. Licsandru, I. Kocsis, Y. X. Shen, S. Murail, Y. M. Legrand, A. van der Lee, D. Tsai, M. Baaden, M. Kumar, M. Barboiu, *J. Am. Chem. Soc.* **2016**, *138*, 5403 – 5409.
[17] M. Barboiu, Y. Le Duc, A. Gilles, P. A. Cazade, M. Michau, Y. M. Legrand, A. van der Lee, B. Coasne, P. Parvizi, J. Post, T. Fyles, *Nat. Commun.* **2014**, *5*, 4142.
[18] J. R. Werber, C. O. Osuji, M. Elimelech, *Nat. Rev. Mater.* **2016**, *1*, 16018.
[19] R. Sengur-Tasdemir, H. E. Tutuncu, N. Gul-Karaguler, E. Ates-Genceli, I. Koyuncu, *Biomimetic Membranes as an Emerging Water Filtration Technology, Biomimetic Lipid Membranes: Fundamentals, Applications, and Commercialization*, (Eds.: F. N. Kök; A. A. Yildiz; F. Inci), Springer, Chem **2019**, pp. 249 – 283.
[20] a) J. Werber, M. Elimelech, *Sci. Adv.* **2018**, *4*, eaar8266; b) P. Wagh, I. C. Escobar, *Environ. Prog.* **2019**, *38*, e13215.
[21] Artificial Water Channels: *Faraday Discuss. 209*, The Royal Society of Chemistry, Cambridge, **2018**.
[22] S. Murail, T. Vasiliu, A. Neamtu, M. Barboiu, F. Sterpone, M. Baaden, *Faraday Discuss.* **2018**, *209*, 125 – 148.
[23] a) I. Kocsis, M. Sorci, H. Vanselous, S. Murail, S. E. Sanders, E. Licsandru, Y. M. Legrand, A. van der Lee, M. Baaden, P. B. Petersen, G. Belfort, M. Barboiu, *Sci. Adv.* **2018**, *4*, eaao5603; b) I. Kocsis, Z. Sun, Y. M. Legrand, M. Barboiu, *NPJ Clean Water* **2018**, *1*, 13.
[24] M. Baaden, M. Barboiu, R. M. Bill, C. L. Chen, J. Davis, M. Di Vincenzo, V. Freger, M. Froba, P. A. Gale, B. Gong, C. Helix-Nielsen, R. Hickey, B. Hinds, J. L. Hou, G. Hummer, M. Kumar, Y. M. Legrand, M. Lokesh, B. Mi, S. Murail, P. Pohl, M. Sansom, Q. Song, W. Song, S. Tornroth-Horsefield, H. Vashisth, M. Vogele, *Faraday Discuss.* **2018**, *209*, 205 – 229.
[25] a) H. Q. Zhao, W. Q. Ong, F. Zhou, X. Fang, X. Y. Chen, S. F. Y. Li, H. Su, N.-J. Chob, H. Q. Zeng, *Chem. Sci.* **2012**, *3*, 2042 – 2046; b) H. Zhao, S. Sheng, Y. Hong, H. Zeng, *J. Am. Chem. Soc.* **2014**, *136*, 14270 – 14276; c) W. Ma, C. Wang, J. Li, K. Zhang, Y.-J. Lu, Y. Huo, H. Zeng, *Org. Biomol. Chem.* **2015**, *13*, 10613 – 10619; d) J. Shen, R. J. Ye, A. Romanies, A. Roy, F. Chen, C. L. Ren, Z. Liu, H. Q. Zeng, *J. Am. Chem. Soc.* **2020**, *142*, 10050 – 10058.
[26] E. Kruse, N. Uehlein, R. Kaldenhoff, *Genome Biol.* **2006**, *7*, 206.
[27] a) K. V. Agrawal, S. Shimizu, L. W. Drahushuk, D. Kilcoyne, M. S. Strano, *Nat. Nanotechnol.* **2017**, *12*, 267 – 273; b) A. I. Kolesnikov, J.-M. Zanotti, C.-K. Loong, P. Thiyagarajan, A. P. Moravsky, R. O. Loutfy, C. J. Burnham, *Phys. Rev. Lett.* **2004**, *93*, 035503; c) Y. Maniwa, K. Matsuda, H. Kyakuno, S. Ogasawara, T. Hibi, H. Kadowaki, S. Suzuki, Y. Achiba, H. Kataura, *Nat. Mater.* **2007**, *6*, 135 – 141.
[28] a) M. Majumder, N. Chopra, R. Andrews, B. J. Hinds, *Nature* **2005**, *438*, 44; b) J. K. Holt, H. G. Park, Y. Wang, M. Stadermann, A. B. Artyukhin, C. P. Grigoropoulos, A. Noy, O. Bakajin, *Science* **2006**, *312*, 1034; c) E. Secchi, S. Marbach, A. Niguès, D. Stein, A. Siria, L. Bocquet, *Nature* **2016**, *537*, 210 – 213; d) Y. Yang, R. Hilmann, Y. Qi, R. Korzetz, N. Biere, D. Emmrich, M. Westphal, B. Buker, A. Hutten, A. Beyer, D. Anselmetti, A. Golzhauser, *Adv. Mater.* **2020**, *32*, 1907850.
[29] G. Hummer, J. C. Rasaiah, J. P. Noworyta, *Nature* **2001**, *414*, 188 – 190.
[30] A. Noy, H. G. Park, F. Fornasiero, J. K. Holt, C. P. Grigoropoulos, O. Bakajin, *Nano Today* **2007**, *2*, 22 – 29.

[31] Z. Siwy, F. Fornasiero, *Science* **2017**, *357*, 753.
[32] J. Geng, K. Kim, J. Zhang, A. Escalada, R. Tunuguntla, L. R. Comolli, F. I. Allen, A. V. Shnyrova, K. R. Cho, D. Munoz, Y. M. Wang, C. P. Grigoropoulos, C. M. Ajo-Franklin, V. A. Frolov, A. Noy, *Nature* **2014**, *514*, 612–615.
[33] R. H. Tunuguntla, F. I. Allen, K. Kim, A. Belliveau, A. Noy, *Nat. Nanotechnol.* **2016**, *11*, 639–644.
[34] R. H. Tunuguntla, R. Y. Henley, Y. C. Yao, T. A. Pham, M. Wanunu, A. Noy, *Science* **2017**, *357*, 792–796.
[35] V. Freger, *Faraday Discuss.* **2018**, *209*, 371–388.
[36] a) V. Percec, A. E. Dulcey, V. S. Balagurusamy, Y. Miura, J. Smidrkal, M. Peterca, S. Nummelin, U. Edlund, S. D. Hudson, P. A. Heiney, H. Duan, S. N. Magonov, S. A. Vinogradov, *Nature* **2004**, *430*, 764–768; b) M. S. Kaucher, M. Peterca, A. E. Dulcey, A. J. Kim, S. A. Vinogradov, D. A. Hammer, P. A. Heiney, V. Percec, *J. Am. Chem. Soc.* **2007**, *129*, 11698–11699.
[37] B. L. de Groot, D. P. Tieleman, P. Pohl, H. Grubmüller, *Biophys. J.* **2002**, *82*, 2934–2942.
[38] X. Zhou, G. Liu, K. Yamato, Y. Shen, R. Cheng, X. Wei, W. Bai, Y. Gao, H. Li, Y. Liu, F. Liu, D. M. Czajkowsky, J. Wang, M. J. Dabney, Z. Cai, J. Hu, F. V. Bright, L. He, X. C. Zeng, Z. Shao, B. Gong, *Nat. Commun.* **2012**, *3*, 949.
[39] B. Gong, *Faraday Discuss.* **2018**, *209*, 415–427.
[40] T. Ogoshi, S. Kanai, S. Fujinami, T.-A. Yamagishi, Y. Nakamoto, *J. Am. Chem. Soc.* **2008**, *130*, 5022–5023.
[41] T. Ogoshi, T.-A. Yamagishi, Y. Nakamoto, *Chem. Rev.* **2016**, *116*, 7937–8002.
[42] W. Si, X.-B. Hu, X.-H. Liu, R. Fan, Z. Chen, L. Weng, J.-L. Hou, *Tetrahedron Lett.* **2011**, *52*, 2484–2487.
[43] a) W. Si, P. Xin, Z. T. Li, J. L. Hou, *Acc. Chem. Res.* **2015**, *48*, 1612–1619; b) X. B. Hu, Z. Chen, G. Tang, J. L. Hou, Z. T. Li, *J. Am. Chem. Soc.* **2012**, *134*, 8384–8387■■Double with Ref. 14. Please replace or delete and renumber■■.
[44] W. Si, L. Chen, X.-B. Hu, G. Tang, Z. Chen, J.-L. Hou, Z.-T. Li, *Angew. Chem. Int. Ed.* **2011**, *50*, 12564–12568; *Angew. Chem.* **2011**, *123*, 12772–12776.
[45] L. Chen, W. Si, L. Zhang, G. Tang, Z. T. Li, J. L. Hou, *J. Am. Chem. Soc.* **2013**, *135*, 2152–2155.
[46] Y. X. Shen, W. Si, M. Erbakan, K. Decker, R. De Zorzi, P. O. Saboe, Y. J. Kang, S. Majd, P. J. Butler, T. Walz, A. Aksimentiev, J. L. Hou, M. Kumar, *Proc. Natl. Acad. Sci. USA* **2015**, *112*, 9810–9815.
[47] a) Y. X. Shen, W. Song, D. R. Barden, T. Ren, C. Lang, H. Feroz, C. B. Henderson, P. O. Saboe, D. Tsai, H. Yan, P. J. Butler, G. C. Bazan, W. A. Phillip, R. J. Hickey, P. S. Cremer, H. Vashisth, M. Kumar, *Nat. Commun.* **2018**, *9*, 2294; b) C. Lang, D. Ye, W. Song, C. Yao, Y.-M. Tu, C. Capparelli, J. A. LaNasa, M. A. Hickner, E. W. Gomez, E. D. Gomez, R. J. Hickey, M. Kumar, *ACS Nano* **2019**, *13*, 8292–8302.
[48] Q. Li, X. Li, L. Ning, C.-H. Tan, Y. Mu, R. Wang, *Small* **2019**, *15*, 1804678.
[49] W. Song, H. Joshi, R. Chowdhury, J. S. Najem, Y. X. Shen, C. Lang, C. B. Henderson, Y. M. Tu, M. Farell, M. E. Pitz, C. D. Maranas, P. S. Cremer, R. J. Hickey, S. A. Sarles, J. L. Hou, A. Aksimentiev, M. Kumar, *Nat. Nanotechnol.* **2020**, *15*, 73–79.
[50] D. H. Zhao, J. Liu, J. W. Jiang, *J. Membr. Sci.* **2019**, *573*, 177–183.
[51] A. Noy, M. Wanunu, *Nat. Nanotechnol.* **2020**, *15*, 9–10.
[52] D. Strilets, S. Fa, T. Ogoshi, M. Barboiu, *Angew. Chem. Int. Ed.* **2020**, https://doi.org/10.1002/anie.202009219; *Angew. Chem.* **2020**, https://doi.org/10.1002/ange.202009219.■■any news?■<?
[53] a) M. Barboiu, S. Cerneaux, A. van der Lee, G. Vaughan, *J. Am. Chem. Soc.* **2004**, *126*, 3545–3550; b) M. Michau, M. Barboiu, *J. Mater. Chem.* **2009**, *19*, 6124–6131.
[54] a) Y. M. Legrand, M. Barboiu, *Chem. Rec.* **2013**, *13*, 524–538; b) M. Barboiu, *Eur. J. Inorg. Chem.* **2015**, 1112–1125.
[55] J. E. Cadotte, US Patent 4277344 A.C, **1981**.

Manuscript received: July 24, 2020
Revised manuscript received: September 3, 2020
Accepted manuscript online: September 11, 2020
Version of record online: ■■ ▮▮, 0000

REVIEW

Desalination

*L.-B. Huang, M. Di Vincenzo, Y. Li, M. Barboiu**

■■ – ■■

Artificial Water Channels: Towards Biomimetic Membranes for Desalination

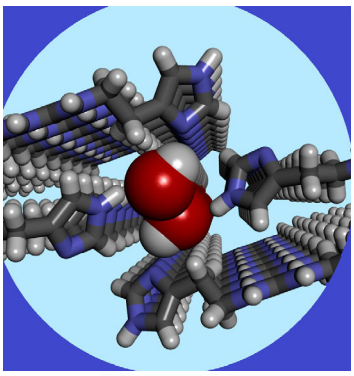

Desalination membranes: The prime objective of Artificial Water Channels (AWC) is to explore the naturally evolved water translocation pathways and assess the possibilities of using them as the basis for 'engineered' desalination processes of enhanced performance. This review proposes to find an easily scalable AWC approach that could be immediately applied to desalination systems to increase their energy efficiency.

Aquaporins (AQPs) are biological water channels known for fast water transport, with complete ion exclusion. Artificial water channels (AWCs) have been designed to mimic the high water permeability and to reject ions at a significant level in bilayer membranes. This Review by M. Barboiu et al. on page ■■ ff. discuss the incipient developments of the first bioimetic membranes and their water filtration performances using AWCs and natural strategies to implement new paradigms for desalination.

Artificial Water Channels are used to explore the naturally evolved water translocation pathways and as the basis for 'engineered' desalination processes of enhanced performance SPACE RESERVED FOR IMAGE AND LINK

Share your work on social media! *Chemistry - A European Journal* has added Twitter as a means to promote your article. Twitter is an online microblogging service that enables its users to send and read text-based messages of up to 140 characters, known as "tweets". Please check the pre-written tweet in the galley proofs for accuracy. Should you or your institute have a Twitter account, please let us know the appropriate username (i.e., @accountname), and we will do our best to include this information in the tweet. This tweet will be posted to the journal's Twitter account @ChemEurJ (follow us!) upon online publication of your article, and we recommended you to repost ("retweet") it to alert other researchers about your publication.

Please check that the ORCID identifiers listed below are correct. We encourage all authors to provide an ORCID identifier for each coauthor. ORCID is a registry that provides researchers with a unique digital identifier. Some funding agencies recommend or even require the inclusion of ORCID IDs in all published articles, and authors should consult their funding agency guidelines for details. Registration is easy and free; for further information, see http://orcid.org/.

Li-Bo Huang
Maria Di Vincenzo
Dr. Yuhao Li
Dr. Mihail Barboiu http://orcid.org/0000-0003-0042-9483

These are not the final page numbers!